ISSN 0036-0244, Russian Journal of Physical Chemistry A, 2019, Vol. 93, No. 11, pp. 2140–2145. © Pleiades Publishing, Ltd., 2019.
Russian Text © The Author(s), 2019, published in Zhurnal Fizicheskoi Khimii, 2019, Vol. 93, No. 11, pp. 1661–1667.

Ethane Oxidation in the Presence of Copper-Containing Zirconia Modified with Acid Additives

P. A. Donyush[a], **A. L. Kustov**[a,b,*], **V. D. Nissenbaum**[b], **A. L. Tarasov**[b], **and L. M. Kustov**[a,b]

[a] *Department of Chemistry, Moscow State University, Moscow, 119991 Russia*
[b] *Zelinsky Institute of Organic Chemistry, Russian Academy of Sciences, Moscow, 119991 Russia*
**e-mail: kyst@list.ru*

Received November 1, 2018; revised March 8, 2019; accepted March 12, 2019

Abstract—The complete oxidation of ethane in the presence of catalysts containing 1, 3, and 5 wt % CuO deposited on four supports (zirconia, sulfated zirconia, tungstated zirconia, and La_2O_3-stabilized zirconia) is studied. The supports and the catalysts are characterized via BET, XRD, and thermal analysis. It is shown that 100% conversion of ethane is achieved even at a temperature of 300°C. It is found that the temperature of 100% conversion falls upon an increase in the copper content; the lowest temperature is obtained for catalysts based on unmodified zirconia. With respect to catalytic activity, the samples with the highest copper content are in the order $5\%Cu/ZrO_2 > 5\%Cu/5\%La_2O_3/ZrO_2 > 5\%Cu/15\%WO_3/ZrO_2 > 5\%Cu/5\%SO_4/ZrO_2$. The temperatures of 100% ethane conversion for these catalysts are 305, 385, 410, and 419°C, respectively.

Keywords: ethane oxidation, alkane oxidation, zirconia, sulfated zirconia, tungstated zirconia, copper oxide

DOI: 10.1134/S0036024419110086

INTRODUCTION

Volatile organic compounds (VOCs) constitute a large group of organic substances that include halogen-containing hydrocarbons, aldehydes, alcohols, aromatic hydrocarbons, alkanes, alkenes, ketones, ethers, and esters [1]. Many VOCs are carcinogenic or greenhouse gases that are responsible for the depletion of the ozone layer and photochemical smog [2]. The control and neutralization of VOC emissions are therefore problems of great concern. Oxidation reactions are commonly used to remove organic substances. Thermal oxidation at temperatures above 900°C is typically used to neutralize VOCs. In industry, however, thermal oxidation is gradually being replaced by catalytic oxidation, which can be employed at much lower temperatures (generally below 500°C) [3].

Catalysts containing noble metals (e.g., Pt, Pd, Rh, and Au) exhibit high efficiency in the oxidation of VOCs at low temperatures [4, 5]. Their disadvantages are high cost, deactivation caused by the sintering of the active phase particles, and poisoning with sulfur compounds [3]. An alternative to metal catalysts is metal oxides, both individual and deposited on different supports; combinations of metal oxides; and such complex oxides as perovskites [6–8]. Supported catalysts are more effective in the complete oxidation of organic compounds, due to the dispersion of the active component [3]. Transition and rare-earth elements are used in this case. Oxides of copper, manganese, iron, nickel, chromium, and cobalt are most commonly used in industry [9–12]. Metal oxide catalysts are less active than noble metals, but they are characterized by low cost and regenerability [3].

Copper oxide is a highly efficient catalyst for the complete oxidation of CO, methane [12], ethanol, acetaldehyde, diesel soot [13], and other organic compounds [14]. Lattice oxygen O^{2-} in CuO plays an important role in oxidative reactions [14]. It was shown in [15] that copper-containing catalysts exhibit high activity in the complete oxidation of a number of hydrocarbons, particularly toluene. Copper oxide is typically deposited on supports with large surface areas, e.g., CeO_2, ZrO_2, and zeolites. According to the literature, the most commonly used supports for CuO are Al_2O_3, CeO_2, ZrO_2, and Ce–Zr-based solid solutions [14]. The most interesting support is zirconia [16].

Zirconia is more effective in its so-called stabilized form, which is obtained by doping zirconia with oxides of metals and nonmetals (SiO_2, La_2O_3, CaO, Y_2O_3, Ce_2O_3) to form a solid solution with ZrO_2 [15]. This stabilization results in the crystallization of zirconia in the tetragonal phase, the specific surface area of which is larger than that of the more thermodynamically stable monoclinic phase. It is known that in oxidative catalysis, the best zirconia promoters are yttrium oxide Y_2O_3 and lanthanum oxide La_2O_3. Adding these oxides substantially increases the number of anion vacancies and thus the adsorbability of oxygen. The content of 1–10 mol % of Y_2O_3/La_2O_3 in zirconia ensures the maximum ionic conductivity [15].

Another effective way of modifying the surface of zirconia is to promote it with sulfate ions SO_4^{2-} and tungstate ions WO_4^{2-} to form so-called solid superacids. The stabilization of zirconia and an increase in the ZrO_2 surface area are in this case observed. Studies of these systems show that in with a number of metal oxides (particularly ZrO_2), such promotion increases their catalytic activity, which exceeds that of 100% sulfuric acid in classical acid catalysis reactions [17]. There are few published data on using solid superacids in the complete oxidation of VOCs. The authors of [4] studied the complete oxidation of methane in the presence of sulfated zirconia with supported platinum, but it was not compared to using a nonsulfated support to confirm the appropriateness of modifying it for this reaction.

In this work, we studied the complete oxidation of a model VOC (ethane) in the presence of catalysts containing 1, 3, and 5 wt % CuO supported on zirconia, sulfated zirconia, tungstated zirconia, and lanthanum oxide-stabilized ZrO_2.

EXPERIMENTAL

Sample Synthesis Procedure

The following reactants were used to synthesize our samples: zirconyl nitrate $ZrO(NO_3)_2 \cdot H_2O$ (Acros, 99%), copper nitrate $Cu(NO_3)_2 \cdot 3H_2O$ (Acros, 99%), lanthanum nitrate $La(NO_3)_3 \cdot 6H_2O$ (Acros, 99%), ammonium paratungstate $(NH_4)_{10}[H_2W_{12}O_{42}] \cdot 4H_2O$ (Acros, 99%), a 25% aqueous solution of ammonia $NH_3 \cdot H_2O$ (Acros, reagent grade), and a concentrated sulfuric acid H_2SO_4 (Khimmed, reagent grade). Zirconia was synthesized as described in [18]. A 0.5 M solution of zirconyl nitrate $ZrO(NO_3)_2$ was prepared. Under vigorous stirring, a 25% aqueous solution of ammonia $NH_3 \cdot H_2O$ was added dropwise to the prepared solution to a pH 8.4. The resulting zirconium hydroxide gel $Zr(OH)_4 \cdot xH_2O$ was dried for 24 h at 120°C and calcined for 4 h at 400°C.

Sulfated zirconia SO_4/ZrO_2 was synthesized as described in [19]. Zirconium hydroxide was repeatedly subjected to incipient wetness impregnation with a 1 M solution of sulfuric acid to ensure a sulfate anion content in the resulting sample of 5 wt %. The sample was then dried for 24 h at 120°C and calcined for 4 h at 650°C. The WO_3/ZrO_2 system was synthesized as described in [20]. A weighed portion of ammonium paratungstate $(NH_4)_{10}[H_2W_{12}O_{42}] \cdot 4H_2O$ was dissolved in distilled water under heating to 70°C and vigorous stirring. The resulting solution was used for the incipient wetness impregnation of zirconium hydroxide. The sample was then dried for 24 h at 120°C and calcined for 4 h at 750°C. The synthesized sample contained 15 wt % tungstate anions. Lanthana-stabilized zirconia was prepared next. A weighed portion of lanthanum nitrate $La(NO_3)_3 \cdot 6H_2O$ was dissolved in distilled water. Zirconium hydroxide was then subjected to incipient wetness impregnation with the solution, dried for 24 h at 120°C, and calcined for 4 h at 400°C. The synthesized sample contained 5 wt % La_2O_3.

The copper-containing catalysts were synthesized next. Three aqueous solutions of copper nitrate were prepared to deposit 1, 3, and 5 wt % of the metal, respectively, on each of the synthesized supports, i.e., ZrO_2, $5\%SO_4/ZrO_2$, $15\%WO_3/ZrO_2$, and $5\%La_2O_3/ZrO_2$. These solutions were used for the incipient wetness impregnation of each of the supports, which were subsequently dried for 24 h at 120°C and calcined for 4 h at 400°C. The powders of the synthesized samples were compressed into pellets under a pressure of 15 MPa and fractionated; a fraction with particle sizes of 0.25–0.5 mm was used in our catalytic test.

Investigation Procedures

Thermal analysis was performed on a MOM Derivatograph-C instrument. A 100-mg weighed portion was placed in an alundum crucible. Thermogravimetry–differential thermogravimetry–differential thermal analysis (TG–DTG–DTA) curves were recorded while linearly raising the temperature from 20 to 800°C at a rate of 10 K/min in air. The reference was α-Al_2O_3. X-ray diffraction analysis was performed on a DRON-2 diffractometer using CuK_α radiation (λ = 1.514 Å). The samples were scanned in the range of $2\theta = 20°–70°$ at a rate of 1 deg/min. The specific surface area was calculated using the Brunauer–Emmett–Teller (BET) approach, according to air adsorption isotherms recorded at 77 K [21].

Catalytic Testing Procedure

The catalytic activity of the samples in the ethane oxidation reaction was determined in a fixed-bed flow reactor under atmospheric pressure. A catalyst sample (0.5 g) was loaded into the reactor in the form of a fraction of 0.25–0.5 mm; a stream of the reaction mixture containing 22.2 vol % of ethane and 77.8 vol % of oxygen was fed to the catalyst at room temperature. The O_2/C_2H_6 molar ratio was 3.5, which corresponds to the stoichiometry of the complete oxidation of ethane: $C_2H_6 + 3.5O_2 = 2CO_2 + 3H_2O$. The feed space velocity of the mixture was 5000 h^{-1}. The reactor was then heated in the temperature-programmed mode; the gas composition at the outlet of the reactor was analyzed via chromatography while raising the temperature in the catalyst bed. The gaseous conversion

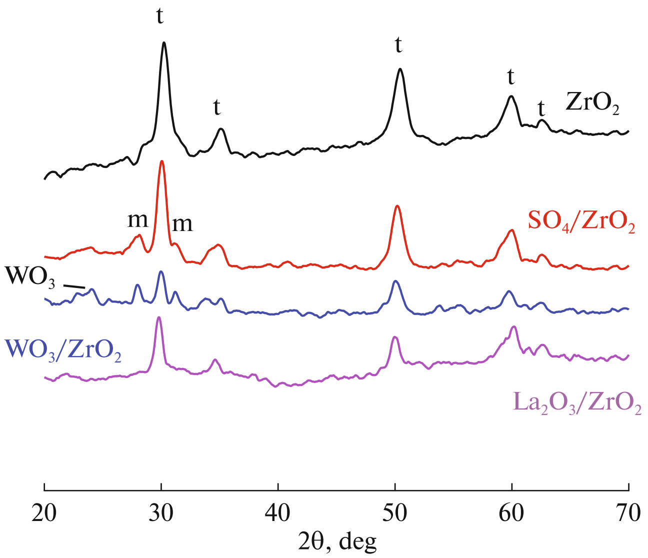

Fig. 1. (Color online) X-ray diffraction patterns of our ZrO_2-based supports.

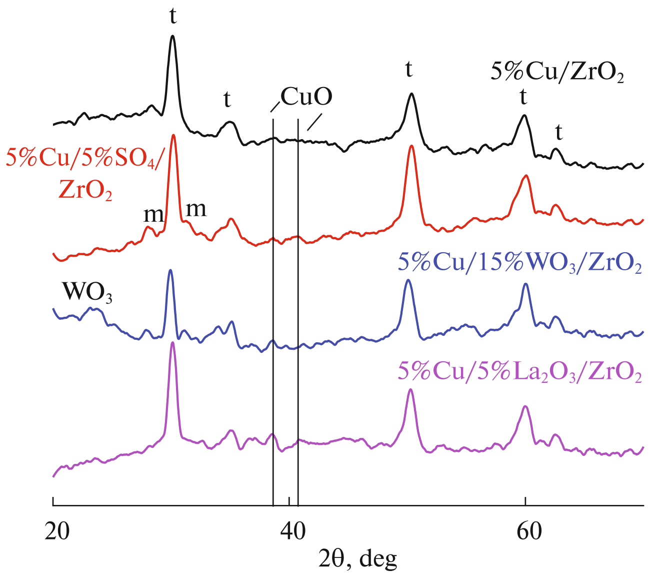

Fig. 2. (Color online) Diffraction patterns of the catalysts containing 5% Cu.

products were analyzed on an M-3700 gas chromatograph equipped with a thermal conductivity detector and a 2-m-long HayeSep-Q packed column in the isothermal mode at a temperature of 60°C.

RESULTS AND DISCUSSION

Physicochemical Properties of the Supports and Catalyst

The synthesized supports and 5% copper-containing catalysts were characterized via powder X-ray diffraction. Figure 1 shows the diffraction patterns of the four synthesized supports, ZrO_2, $5\%SO_4/ZrO_2$, $15\%WO_3/ZrO_2$, and $5\%La_2O_3/ZrO_2$. In all cases, a mixture of monoclinic (with diffraction peaks at $2\theta = 28.17°$ and $31.46°$) and tetragonal ZrO_2 phases (with diffraction peaks at $2\theta = 30.27°$, $35.25°$, $50.37°$, $60.20°$, and $62.96°$) is seen. The diffraction patterns of sulfated zirconia and lanthanum oxide-promoted zirconia are almost identical to the diffraction pattern of ZrO_2. The diffraction pattern does not exhibit reflections characteristic of sulfates. The authors of [17] showed that supported sulfate anions cannot be detected by these means. Lanthanum oxide is presumably in the X-ray amorphous state. The diffraction pattern of the $15\%WO_3/ZrO_2$ sample exhibits reflections characteristic of the WO_3 tungsten oxide phase (with peaks at $2\theta = 22°$ and $24.03°$). Figure 2 shows the diffraction patterns of the catalysts containing 5% Cu. Reflections that can be attributed to copper oxide CuO are identified (with peaks at $2\theta = 38.47°$ and $42.20°$) for all the samples.

Figure 3 compares derivatograms of zirconium hydroxide and zirconium hydroxide impregnated with sulfuric acid. The total weight loss of freshly prepared zirconium hydroxide upon heating from 20 to 800°C was 22%. The weight loss occurs in several stages. At the first stage, below 200°C, the adsorbed water is removed [22]; ammonium nitrate then decomposes, which apparently corresponds to the peak in the DTG curve at 265°C and the slight exothermic effect [23]. Finally, in the temperature range of 300–400°C, coor-

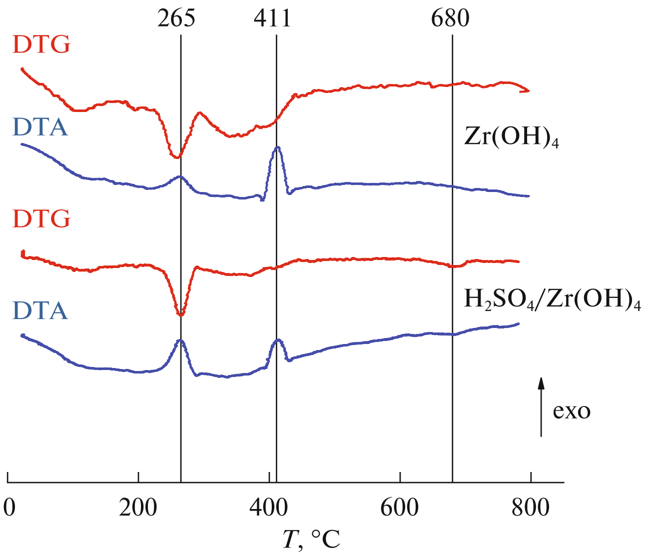

Fig. 3. (Color online) Derivatograms of $Zr(OH)_4$ and $H_2SO_4/Zr(OH)_4$.

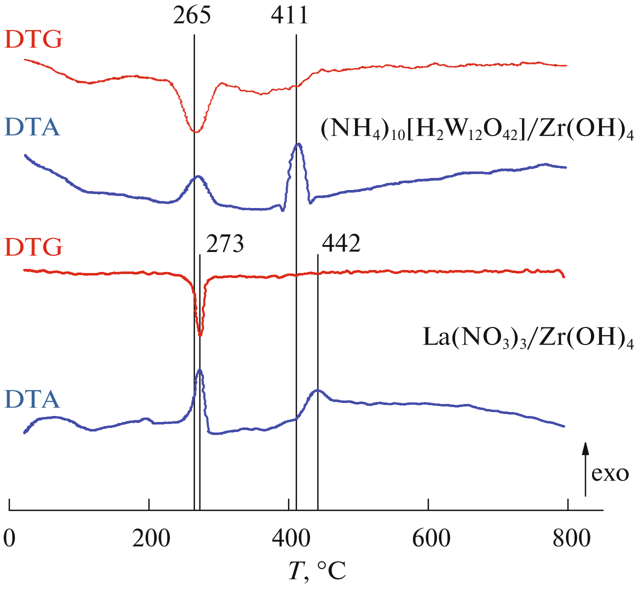

Fig. 4. (Color online) Derivatograms of $(NH_4)_{10}[H_2W_{12}O_{42}]/Zr(OH)_4$ and $La(NO_3)_3/Zr(OH)_4$.

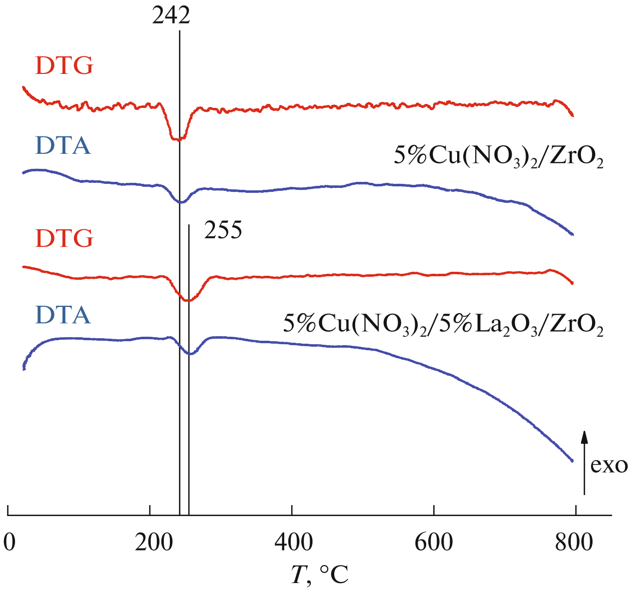

Fig. 5. (Color online) Derivatograms of $Cu(NO_3)_2/ZrO_2$ and $Cu(NO_3)_2/5\%La_2O_3/ZrO_2$.

dinated water is split off [22] and zirconia ZrO_2 is crystallized, which corresponds to the pronounced exothermic effect at 410°C [18]. The total weight loss of freshly prepared zirconium hydroxide impregnated with sulfuric acid upon heating from 20 to 800°C was 26.5%. The DTG curve recorded for zirconium hydroxide impregnated with sulfuric acid is generally similar to the above DTG curve of zirconium hydroxide. The difference is that at 680°C, the DTG-curve exhibits a peak without a pronounced heat effect that presumably corresponds to the removal of deposited sulfur in the form of SO_3 [24].

Figure 4 shows derivatograms of zirconium hydroxide impregnated with ammonium paratungstate and lanthanum nitrate. In the first case, the total weight loss was 21.2%. The behavior of the DTG-curve of zirconium hydroxide impregnated with ammonium paratungstate is generally similar to the behavior of the curve for zirconium hydroxide. The difference is that, in a temperature range of 240–320°C, $(NH_4)_{10}[H_2W_{12}O_{42}]$ undergoes decomposition to form ammonia and WO_3 [25]. In the second case, the total weight loss was 34.5%. The DTG curve of zirconium hydroxide impregnated with lanthanum nitrate clearly shows a peak at 273°C, accompanied by an exothermic effect. In other respects, the behavior of the curve is similar to that of zirconium hydroxide.

Figure 5 shows derivatograms of zirconia and lanthanated zirconia impregnated with copper nitrate. The total weight loss is 5.2 and 5.5%, respectively. The DTG curves exhibit peaks with temperatures at the maximum of 242 and 255°C, which we attribute to the removal of weakly bound water and crystalline hydrate water from $Cu(NO_3)_2 \cdot 3H_2O$ and the subsequent decomposition of copper nitrate. These processes are accompanied by an endothermic effect.

The specific surface areas of the original zirconium hydroxide, the four synthesized supports, and the 5% copper-containing catalysts were determined via low-temperature nitrogen adsorption; the results are shown in Table 1. It is evident from the table that unmodified zirconia had the largest specific surface area. The results correlate with the temperatures of calcination during the synthesis of the samples. With $5\%SO_4/ZrO_2$ and $15\%WO_3/ZrO_2$, the temperatures of calcination were 650 and 750°C, respectively. These results suggest the deposition of copper leads to a slight reduction in the specific surface area of the support.

Table 1. Specific surface area (S_{BET}, m^2/g) of the supports and the catalysts based on them

Sample	S_{BET}
$Zr(OH)_4$	56.6
ZrO_2	37.0
$5\%Cu/ZrO_2$	29.2
$5\%SO_4/ZrO_2$	27.1
$5\%Cu/5\%SO_4/ZrO_2$	19.6
$15\%WO_3/ZrO_2$	15.7
$5\%Cu/15\%WO_3/ZrO_2$	9.9
$5\%La_2O_3/ZrO_2$	24.6
$5\%Cu/5\%La_2O_3/ZrO_2$	17.3

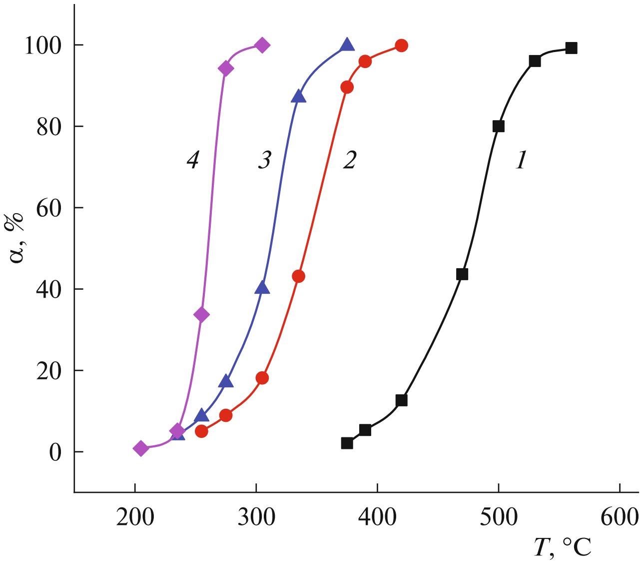

Fig. 6. (Color online) Temperature dependences of ethane conversion (α) in the presence of samples (*1*) ZrO_2, (*2*) $1\%Cu/ZrO_2$, (*3*) $3\%Cu/ZrO_2$, and (*4*) $5\%Cu/ZrO_2$.

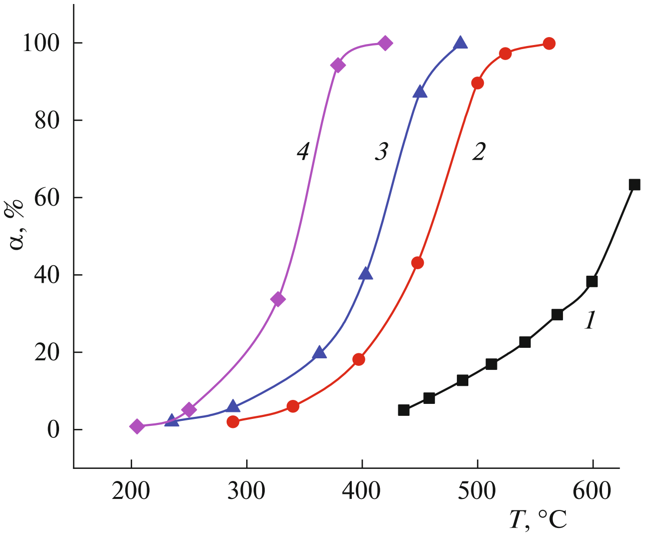

Fig. 7. (Color online) Temperature dependences of ethane conversion (α) in the presence of samples (*1*) $5\%SO_4/ZrO_2$, (*2*) $1\%Cu/5\%SO_4/ZrO_2$, (*3*) $3\%Cu/5\%SO_4/ZrO_2$, and (*4*) $5\%Cu/5\%SO_4/ZrO_2$.

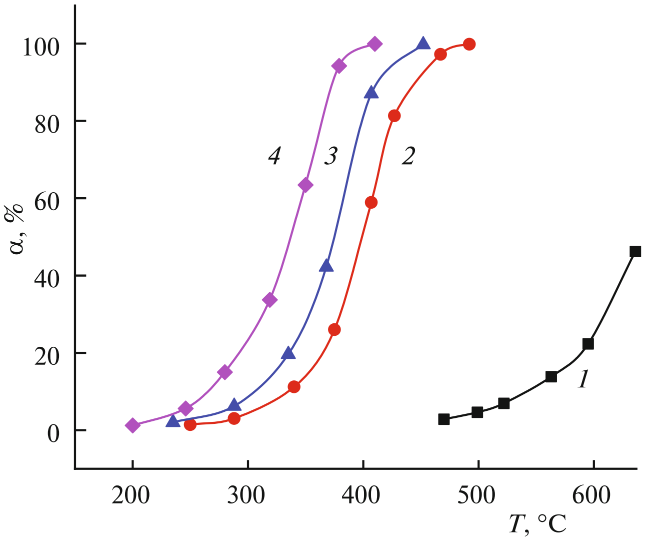

Fig. 8. (Color online) Temperature dependences of ethane conversion (α) in the presence of the samples: (*1*) $15\%WO_3/ZrO_2$, (*2*) $1\%Cu/15\%WO_3/ZrO_2$, (*3*) $3\%Cu/15\%WO_3/ZrO_2$, and (*4*) $5\%Cu/15\%WO_3/ZrO_2$.

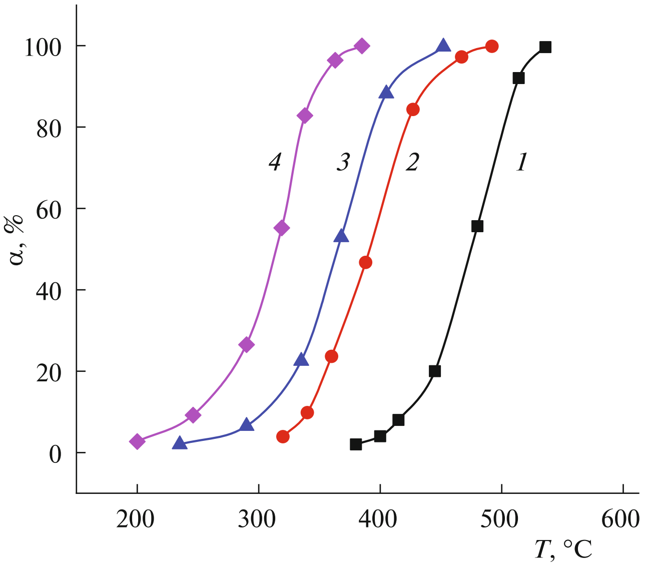

Fig. 9. (Color online) Temperature dependences of ethane conversion (α) in the presence of the samples: (*1*) $5\%La_2O_3/ZrO_2$, (*2*) $1\%Cu/5\%La_2O_3/ZrO_2$, (*3*) $3\%Cu/5\%La_2O_3/ZrO_2$, and (*4*) $5\%Cu/5\%La_2O_3/ZrO_2$.

This can be attributed to CuO occupying pores in the structure of the substrate and the particles sintering during recalcination.

Catalytic Oxidation of Ethane

Figure 6 shows the temperature dependences of ethane conversion for samples ZrO_2, $1\%Cu/ZrO_2$, $3\%Cu/ZrO_2$, and $5\%Cu/ZrO_2$. The results show that 100% ethane conversion was achieved in all cases. The temperature of the reaction's ignition in the presence of pure zirconia was 375°C. The deposition of copper lowered the temperature of the reaction's ignition and those of 50 and 100% conversion.

Figure 7 shows the temperature dependences of ethane conversion for samples $5\%SO_4/ZrO_2$, $1\%Cu/5\%SO_4/ZrO_2$, $3\%Cu/5\%SO_4/ZrO_2$, and $5\%Cu/5\%SO_4/ZrO_2$. The results show that for the copper-containing catalysts, 100% ethane conversion was achieved in all cases under our test conditions. However, the catalytic activity was considerably lower for the support (sulfated zirconia): ethane conversion was as low as 85% under our temperature conditions ($T_{\max} = 650°C$). The deactivation of sulfated zirconia that was described in [17] was thus observed. The deposition of copper substantially lowered the temperature of the reaction's ignition and those of 50 and 100% conversion.

Figure 8 shows the conversion curves for samples $15\%WO_3/ZrO_2$, $1\%Cu/15\%WO_3/ZrO_2$, $3\%Cu/15\%WO_3/ZrO_2$, and $5\%Cu/15\%WO_3/ZrO_2$. It is evident that 100% ethane conversion was achieved for all copper-containing catalysts under our test conditions. As in the case above, the support (tungstated zirconia) exhibited an extremely low catalytic activity. At $T = 650°C$, ethane conversion was as low as 50%. The deactivation of tungstated zirconia corresponds to the data of [17]. Although this support was less active than sulfated zirconia, this set of copper catalysts exhibited slightly higher activity.

Figure 9 shows conversion curves for the set of lanthanum-containing samples: $5\%La_2O_3/ZrO_2$, $1\%Cu/5\%La_2O_3/ZrO_2$, $3\%Cu/5\%La_2O_3/ZrO_2$, and $5\%Cu/5\%La_2O_3/ZrO_2$. The results show that 100% ethane conversion was achieved in all cases under our test conditions. Lanthanated zirconia as a support is better than the two previous supports, but it is inferior to unmodified zirconia. The catalytic activity of this set of copper-containing catalysts is also higher than the activity of the two sets above, but it is inferior to the activity of the first set. With respect to catalytic activity, the samples are in the order $5\%Cu/ZrO_2$ > $5\%Cu/5\%La_2O_3/ZrO_2$ > $5\%Cu/15\%WO_3/ZrO_2$ > $5\%Cu/5\%SO_4/ZrO_2$. The temperatures of 100% ethane conversion are 305, 385, 410, and 419°C, respectively.

CONCLUSIONS

It was found that the highest activity in the ethane oxidation reaction is exhibited by catalysts based on unmodified zirconia. This can be attributed to the larger specific surface area of these samples. It was shown via BET, XRD, and TG–DTA that the sulfation and tungstation of zirconia stabilize the tetragonal phase of zirconia, as does adding lanthanum to it. The decomposition of the initial compounds and the crystallization of zirconia are observed below 410°C. In addition, we may assumed that copper oxide deposited on modified supports reacts with additives to form sulfate, tungstate, or cuprate, which are less active than copper oxide.

REFERENCES

1. F. J. Janssen and R. A. Santen, *Environmental Catalysis* (Imperial College Press, London, 1999).
2. L. Matejova, P. Topka, K. Jiratova, and O. Solcova, Appl. Catal. A: Gen. **443**, 40 (2012).
3. M. S. Kamal, S. A. Razzak, and M. M. Hossain, Atmos. Environ. **140**, 117 (2016).
4. L. M. Kustov, K. M. Skupov, S. S. Goryashchenko, and O. V. Masloboishchikova, Zh. Fiz. Khim. **88**, 891 (2014).
5. A. V. Kucherov, O. P. Tkachenko, O. A. Kirichenko, et al., Top. Catal. **52**, 351 (2009).
6. E. V. Makshina, L. V. Borovskikh, A. L. Kustov, G. N. Mazo, and B. V. Romanovskii, Russ. J. Phys. Chem. A **79**, 191 (2005).
7. A. L. Kustov, O. P. Tkachenko, L. M. Kustov, and B. V. Romanovsky, Environ. Int. **37**, 1053 (2011).
8. N. A. Davshan, A. L. Kustov, O. P. Tkachenko, et al., ChemCatChem **6**, 1990 (2014).
9. T. P. Otroshchenko, A. O. Turakulova, V. A. Voblikova, L. V. Sabitova, S. V. Kutsev, and V. V. Lunin, Russ. J. Phys. Chem. A **87**, 1804 (2013).
10. Yu. P. Semushina, S. I. Pechenyuk, L. F. Kuz'mich, and A. I. Knyazeva, Russ. J. Phys. Chem. A **91**, 26 (2017).
11. I. Yu. Kaplin, E. S. Lokteva, E. V. Golubina, K. I. Maslakov, S. A. Chernyak, A. V. Levanov, N. E. Strokova, and V. V. Lunin, Russ. J. Phys. Chem. A **90**, 2157 (2016).
12. K. I. Slovetskaya, A. A. Greish, M. P. Vorob'eva, and L. M. Kustov, Russ. Chem. Bull. Int. Ed. **50**, 1589 (2001).
13. A. N. Pushkin, O. K. Gulish, D. A. Koshcheeva, and M. S. Shebanov, Russ. J. Phys. Chem. A **87**, 23 (2013).
14. Y. Fang and Y. Guo, Chin. J. Catal. **39**, 566 (2018).
15. A. Bialas, T. Kondratovicz, M. Drozdec, and P. Kustrowski, Catal. Today **257**, 144 (2015).
16. G. Aguila, F. Gracia, J. Cortes, and P. Araya, Appl. Catal. B: Environ. **77**, 325 (2008).
17. A. V. Ivanov and L. M. Kustov, Ross. Khim. Zh. **2**, 21 (2000).
18. K. Arata, Adv. Catal. **37**, 165 (1990).
19. A. V. Ivanov, E. G. Khelkovskaya-Sergeeva, and T. V. Vasina, Russ. Chem. Bull. **48**, 1266 (1999).
20. M. Scheifauer, R. Grasselli, and H. Knozinger, Langmuir **14**, 30 (1998).
21. A. L. Klyachko-Gurvich, Izv. Akad. Nauk SSSR, Otd. Khim. Nauk, No. 10, 1884 (1961).
22. A. Clearfield, G. P. D. Serrette, and A. H. Khazi-Syed, Catal. Today **20**, 295 (1994).
23. O. Kirichenko, G. Kapustin, V. Nissenbaum, et al., J. Therm. Anal. Calorim. **134**, 233 (2018).
24. B. Reddy and M. Patil, Chem. Rev. **109**, 2185 (2009).
25. L. P. Kolmakova, O. N. Kovtun, and N. N. Dovzhenko, J. Siber. Fed. Univ., Eng. Technol. **3**, 293 (2010).

Translated by M. Timoshinina